MARKOV CHAIN MONTE CARLO ANALYSIS OF HARMONIZED PHYSIOLOGICALLY-BASED PHARMACOKINETIC MODEL OF TRICHLOROETHYLENE AND ITS METABOLITES

Prepared for:

United States Air Force

Prepared by:

USAF-EPA TCE PBPK workgroup

Oct. 14, 2004

USAF-EPA TCE PBPK workgroup members:

Jerry Blancato: U.S. Environmental Protection Agency (EPA)

Weihsueh Chiu**: U.S. Environmental Protection Agency

Harvey J. Clewell**: ENVIRON Health Sciences Institute, Ruston, Louisiana 71270

Tammie R. Covington: ENVIRON Health Sciences Institute, Ruston, Louisiana 71270

Jeffrey W. Fisher**: University of Georgia, Athens, GA

Eric Hack*: Toxicology Excellence for Risk Assessment (*TERA*)

John Lipscomb**: U.S. Environmental Protection Agency

David R. Mattie: Air Force Research Laboratory (AFRL), the Biosciences Protection Division of the Human Effectiveness Directorate (HEPB)

Miles Okino: U.S. Environmental Protection Agency

Fred Power: U.S. Environmental Protection Agency

Qiyu J. Zhao*: Toxicology Excellence for Risk Assessment

Acknowledgement to Teri Sterner (AFRL/HEPB) for assistance to Jeff Fisher and Eric Hack

*: Primary authors

**: Major contributors

Introduction

Physiologically-based pharmacokinetic (PBPK) models are simplified representations of complex biological systems. Recently, a harmonized PBPK model of trichloroethylene (TCE) and its metabolites was developed by the USAF-EPA TCE PBPK working group. This revised PBPK model was developed using both the toxicokinetic data used previously by Fisher (2000) and Clewell et al. (2000), as well as some more recent data not used in either of the previous efforts. However, this model depends on many underlying factors that vary from individual to individual. In addition to the inter-individual variability and the model error, uncertainty in model predictions arises from uncertain mean parameter values for a population and measurement errors in the data collected to parameterize the models. Therefore, there is an unknown amount of uncertainty in risk estimates based on model predictions derived using nominal, or best estimate, parameter values. To calibrate this newly developed model and quantitatively estimate the uncertainty in the model output, we used Markov Chain Monte Carlo (MCMC) to perform a Bayesian analysis.

A Bayesian approach facilitates the combination of prior information about the parameter values based on the literature and experimental data from whole animal studies to obtain posterior distributions for the parameters (Gilks et al. 1996; Bois 1999, 2000). This approach is particularly well suited for updating model parameterizations with newly available experimental data, or for recalibrating models that have been fit using less sophisticated approaches, such as visual fitting or maximum likelihood estimation for a subset of the parameters (i.e., maximizing data likelihood by varying VMax and KM while holding all other parameters fixed).

Inter-individual variability is estimated separately from the uncertainty in the population mean in a hierarchical population model. A hierarchical population model uses the same PBPK model for all individuals in the population, while parameter distributions are iteratively sampled to provide different model parameters for each individual.

A population model was developed and Bayesian analysis was performed to obtain posterior distributions for the PBPK model parameters. The analysis was performed using MCSIM (Bois and Maszle, 1997), a publicly available implementation of MCMC analysis that is available at (http://toxi.ineris.fr/activites/toxicologie_quantitative/mcsim/mcsim.php#article3). The same version of the software used to analyze the Clewell et al. PBPK model (Bois, 2000) was used for this analysis.

Population Model

The hierarchical population model developed, following Gelman et al. (1996), is shown in Figure 1. At the population level, prior distributions for the population mean (**M**) and the population variance ($\mathbf{S}^2$) are defined for each parameter to be re-estimated in the analysis. Note that these are distributions, not point estimates, reflecting uncertainty in the estimated mean and variability among a population. In the subject level, individual experimental conditions (ϕ), such as doses and body weights, are defined for input to the PBPK model (f). The parameter values used in the PBPK model are determined by random sampling from the distributions (θ) defined by a mean and variance randomly sampled from the population level distributions of **M** and $\mathbf{S}^2$. The experimental data are assumed to be lognormally distributed, and the combined measurement and model errors (σ^2) are modeled using uninformative, log-uniform distributions.

Data

Rat, mouse, and human data were used to recalibrate the model using separate MCMC simulations for each species. The data were obtained from the acslXtreme command file used to develop the harmonized PBPK model, and reformatted for use with MCSim.

The data used in MCMC analysis include studies with various exposure conditions. Bernauer et al. (1996) exposed rats and humans to 40, 80, or 160 ppm TCE via inhalation for 6 hours, and measured the time-course of trichloroacetate (TCA), trichloroethanol glucuronide (TCOG), TCA plus TCOG, and N-acetyl dichlorovinylcysteine (NDCVC) excretion in urine. Prout et al. (1985) exposed mice and rats to 1000 mg/kg TCE in oil

via gavage and measured the time-course of TCE, TCA, and free plus bound trichloroethanol (TCOH) in blood. Templin et al. exposed mice to 500 mg/kg TCE via oral gavage (Templin et al., 1993) and rats to 100 mg/kg TCE via oral gavage (Templin et al., 1995) and measured the time-course of TCE, TCA, and free TCOH in blood. Fisher et al. (1991) exposed rats to 505, 529, and 600 ppm TCE for 4 hours via inhalation, and mice to 110 and 368 ppm for 4 hours, and measured the time-course of TCE and TCA in the animals' blood. Fisher et al. (1991) also conducted closed-chamber experiments where groups of male mice were placed in a chamber containing 1020, 1800, 3800, 5600, and 10000 ppm TCE, and female mice were placed in a chamber containing 300, 700, 1100, 3700, and 7000 ppm TCE; the disappearance of TCE from the chamber was recorded. Andersen et al. (1987) reported data from closed chamber experiments with rats at concentrations of 100, 450, 1000, 2000, and 4640 ppm TCE. Larson and Bull (1992) administered TCE via oral gavage to rats at 200, 600, and 2996 mg/kg doses, and measured the time-course of TCE and TCA in the blood. Greenberg et al. (1999) exposed mice to 100 or 600 ppm TCE via inhalation and measured the time-course of TCE, TCA, and free TCOH in blood. Fisher et al. (1998) exposed individual human volunteers to 50 or 100 ppm TCE via inhalation for 4 hours and measured the time-course of concentrations of TCE, TCA, and free TCOH in blood, and the amount of TCA and free plus bound TCOH excreted in the urine.

Some of the data available from the model development stage were not used in the MCMC analysis of the mouse and human models. The mouse simulations failed to converge to a stationary posterior distribution for several of the model parameters. Upon inspection of the results, it was noted that the Abbas and Fisher (1997) data were the likely source of the problem, though the reason is unclear at this time. These data were removed from the analysis and the simulations were rerun to obtain convergence to a stationary posterior distribution. The number of human data sets was reduced from 34 to 11 due to computational constraints. Many of the data sets overlapped in terms of exposure levels and endpoints measured, so a subset of the data were chosen which included the available data on both the P-450 and glutathione conjugation metabolic pathways. The data of Bernauer et al. (1996) were retained because this study was the

only one to measure a product of the glutathione conjugation pathway, urinary excretion of NDCVC. The data of Fisher et al. (1998) on 2 men and 2 women were retained because this study measured multiple products of oxidative metabolism, these individual volunteers were exposed at multiple concentrations of TCE (50 and 100 ppm), and both men and women subjects were used. Although not all of the data are incorporated into the analysis presently, the Bayesian approach allows subsequent analyses of the remaining data to be performed easily by using the current posterior distributions as prior distributions for further analysis.

The dichloroacetic acid (DCA) data were excluded for all species. DCA is produced from TCA *ex vivo*, making measurements of DCA an unreliable estimate of *in vivo* levels. Due to this analytical difficulty, these data were not included in the analysis.

Figure 1
Illustration of Markov Chain Monte Carlo Approach

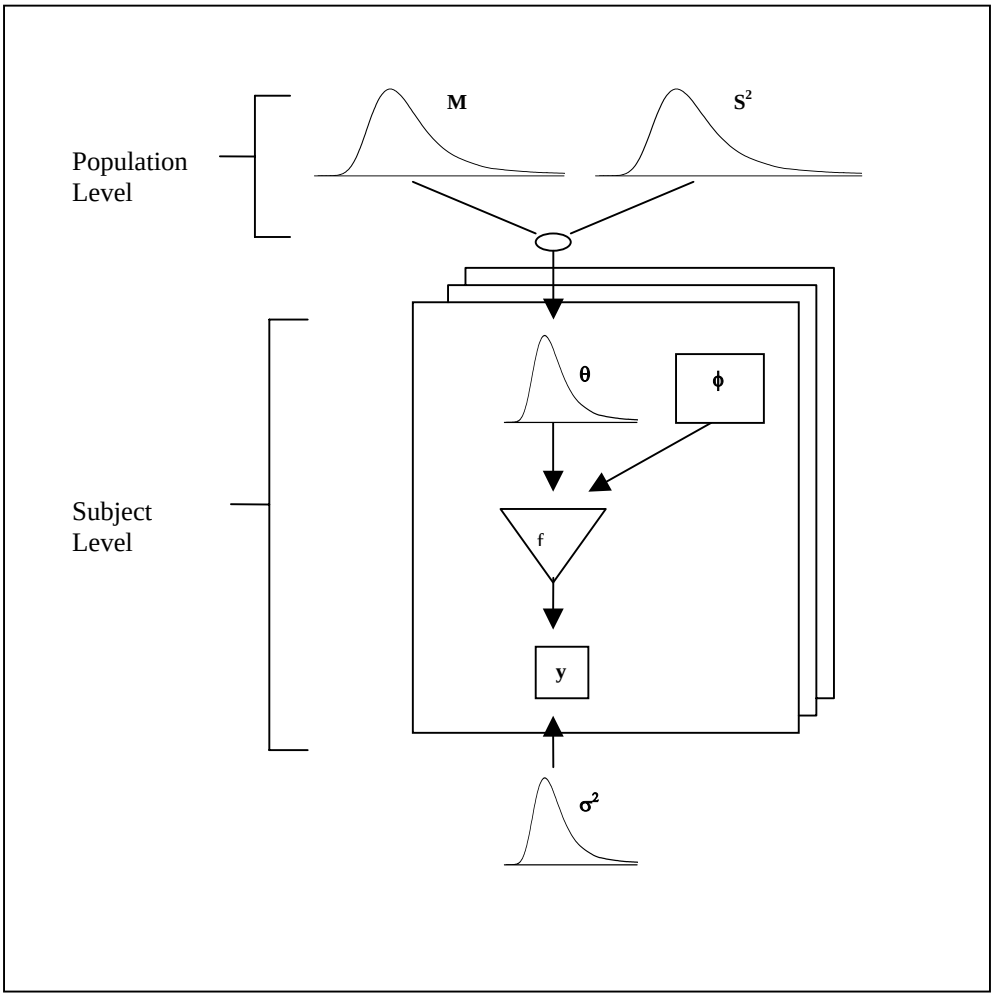

Prior distributions

Prior distributions reflecting the existing knowledge about the parameter distributions based on the scientific literature, defined as described by Bois (2000), are shown in Tables 1, 2, and 3. Population mean distributions (**M**) for blood flows, tissue volumes, volumes of distribution for metabolites, and the plasma:blood ratio were modeled using

normal distributions, with means taken from the PBPK model. All other parameter population means were modeled as lognormal distributions, with geometric means set equal to the values used for model development. The standard deviations (uncertainty in mean) for the mean volumes, blood flows, hematocrit, volumes of distribution, and partition coefficients were set according to the values in Table 1 of Bois (2000). Standard deviations of the mean TCA binding parameters were generously supplied by Dr. Mike Lumpkin in a personal communication. The standard deviations for all other population means were set corresponding to a 200% coefficient of variation, based on methodology used by Bois (2000) to reflect a high degree of uncertainty in the mean. In other words, a 200% coefficient of uncertainty was used for the population means. All mean parameter distributions were bounded to be within 2 prior standard deviations of the mean.

All population standard deviations (**S**) were modeled using an inverse gamma distribution with shape parameter equal to three and inverse scale parameter set equal to $\mathbf{S_0}=\ln(1+CV^2)$, where CV was set at 50% (Bois, 2000). This parameterization corresponds to a vague prior distribution for the standard deviation with a 100% coefficient of uncertainty (Gelman et al., 1996).

The Michaelis-Menten metabolism described in the PBPK model was modified slightly to improve the performance of the Markov Chain Monte Carlo analysis. The metabolism parameters, VMax and KM, are highly correlated, which can lead to slowly mixing chains and make obtaining convergence problematic. To reduce this correlation, prior distributions were defined for the transformation Cl=VMax/KM, and the reverse transformation (VMax=Cl*KM) was performed in the model after sampling from the distribution of Cl. The prior population mean of Cl was distributed log-normally with a geometric mean equal to the ratio of prior geometric means for VMax and KM, and log-scale variance equal to the sum of the log-scale variances of VMax and KM. For the rat and mouse models, the geometric means were set equal to the values used in the development of the PBPK model.

For the oxidative metabolism of TCE in human, the estimates of KM and VMax from *in vitro* hepatocyte data by Lipscomb et al. (1998) were used to compute geometric means and standard deviations of Cl. The VMax and KM were interpreted differently than the values derived during the PBPK model development phase. That is, the *in vitro*–based estimate of VMax has units of mg/hour/kg liver, rather than mg/hour/kg $BW^{3/4}$, and is scaled by the liver mass instead of body weight (BW) to the ¾ power. Furthermore, KM is divided by the liver:blood partition coefficient to correct for the measurement of affinity in a sample of purified hepatocytes.

Following Bois (2000), the prediction error distributions (σ^2) were modeled using log-uniform priors with a lower bound of 0.29 to prevent the error from reaching zero. The 0.29 corresponded to a 30% CV for measurement plus model error.

PBPK Model Adjustments

Some modifications were made to the model to facilitate the varying inputs resulting from the distributional approach. The alveolar ventilation rate was correlated with the cardiac output by replacing the parameter QPC with a ventilation perfusion ratio (VPR) that is the ratio of the ventilation rate to the cardiac output. The fractional blood flows were constrained to sum to unity by sampling for all compartments except for the rapidly perfused tissues, and then setting the blood flow to the rapidly perfused tissues equal to the total cardiac output minus the sum of the flows to the other tissues. Similarly, the volume of the slowly perfused compartment was computed as the 82% of the body weight minus the sum of the volumes of the other tissues.

MCMC Simulation

The analysis of the rat, mouse, and human experiments was performed separately. Convergence was monitored using analysis of variance as described by Gelman (1996). The estimated potential scale reduction, a ratio of an upper bound and a lower bound of the variance in the target distribution, is used to diagnose convergence. In the limit as the number of iterations of the Markov chains goes to infinity, the ratio declines to unity. In

practice, simulation of two or three independent Markov chains is continued until the estimated potential scale reduction is less than 1.2 for the means of all parameters (Gelman, 1996).

In this analysis, three independent chains were run for 25000 iterations for each species, and the last 5000 to 7500 iterations from each chain were taken as the posterior distribution. The convergence criteria were satisfied for all parameters of the human model. For the rat model, the potential scale reduction for VMax/KM and KM were 1.7 and 1.8, respectively. Although additional iterations will be required to obtain potential scale reductions less than 1.2, visual inspection of the chains indicates that they appeared to be converging to the same distribution. For the mouse model, the potential scale reduction of VMax/KM and KM were well above the 1.2 benchmark at 3.9 and 3.2, respectively. This is likely due to slow mixing of these chains, which may be caused by the correlation between these two parameters. Plotting VMax/KM versus KM for one of the mouse runs shows that the parameters are apparently highly, negatively correlated. Two of the three chains were consistent after 25000 iterations, and the third was approaching the other two from above. As a result, the center of the posterior mean distribution is likely underestimated for VMax/KM, and overestimated for KM. Furthermore, the spread of these distributions is likely overestimated. Additional iterations will be required to increase the confidence in these posterior distributions.

The posterior distributions for the rat, mouse, and human model parameters are shown in Tables 1, 2, and 3, respectively. Compared to the prior distributions of the parameter means, the estimated standard deviations (SD) are apparently reduced, indicating a reduced uncertainty in the newly estimated parameters for the PBPK model.

Although this analysis included a large amount of data, some data sets were omitted either due to convergence or computational-time issues. The mouse and rat analyses revealed slow convergence for the VMaxC/KM and KM parameter distributions, apparently due to slow mixing of the chains. This is likely due to large correlations between these parameters, and reparameterizations may help improve the mixing.

Another approach which may improve performance is to fix the population means for the physiological parameters and partition coefficients. This approach may be the most appropriate way to run the simulations for 2 reasons: the physiological parameters and partition coefficient are fairly well-known quantities, and the kinetic data contain information on kinetic parameters, but may not be appropriate for estimating physiological parameters. A variation of this approach would be to fix the populations means for the parameters that are not sensitive. That is to say, the mean blood flow to a tissue, for example, would be fixed if it does not have a significant impact on the levels of TCE or metabolites in the tissues or blood.

For the human model, which did not exhibit the slow mixing that was apparent in the animal models, an additional approach to running the remaining data sets may be useful. The posterior distributions that were obtained from the subset of human data could be used as the prior distributions for a run with the remainder of the data, or a portion of the remaining data. This technique could be repeated with multiple subdivisions of the data until all data were analyzed. This approach is theoretically sound, but in practice, one may need to be cautious of the order in which the data are analyzed. For example, analyzing data from one experiment, followed by data from a second experiment that may have different measurement techniques or biases can cause numerical difficulties resulting in chains that will not converge.

There are issues regarding the estimation of the variability and distinguishing between inter-group and inter-individual variability. Most of the available pharmacokinetic data are mean observations for groups of subjects, and the size of the group varies from study to study. The variability in response and pharmacokinetic parameters from one group to the next, the inter-group variability, is less than inter-individual variation within the group. A method for handling the grouped data in the MCSim algorithm has not been developed, particularly when the grouped data must be combined with individual data or data from groups of a different size.

A related issue is that of modeling serially correlated and serial sacrifice data. Because the model is run through the time-course data with the same vector of parameters after each random selection, serially correlated data are probably modeled properly. Serial sacrifice data are treated similarly, and the inter-experimental variability is estimated. However, the serial sacrifice data should properly be modeled as a separate animal or group of animals for each time point. If the serial sacrifice data are separated in this manner, the intra-experimental variability will have to be addressed as well as the inter-experimental variability.

Our results indicate that MCMC analysis provided significantly improved estimation of parameters for the PBPK model calibration. In addition, the MCMC analysis estimated posterior distributions of the model parameters, providing an important step toward estimating uncertainty of dose-response relationships in noncancer and cancer risk assessment.

References

Abbas R and Fisher JW. 1997. A physiologically based pharmacokinetic model for trichloroethylene and its metabolites, chloral hydrate, trichloroacetate, dichloroacetate, trichloroethanol, and trichloroethanol glucuronide in B6C3F1 mice. Toxicol. Appl. Pharmacol. 147:15-30

Andersen, M.E., Clewell, H.J., Gargas, M.L., Smith, F.A., and Reitz, R.H. 1987. Physiologically based pharmacokinetics and the risk assessment process for methylene chloride. *Toxicol. Appl. Pharmacol.*, 87, 185-205,.

Bernauer, U., Birner, G., Dekant, W., and Henschler, D. 1996. Biotransformation of trichloroethylene: Dose-dependent excretion of 2,2,2-trichlor-metabolites and mercapturic acids in rats and humans after inhalation. *Arch. Toxicol.*, 70(6), 338-346.

Bois, F. 1999. Analysis of PBPK Models for Risk Characterization. *Ann. NY Acad. Sci.* 895:317-337.

Bois, F. 2000. Statistical Analysis of Clewell et al. PBPK Model of Trichloroethylene Kinetics. *Environ. Health Perspect.* 108(2):307-316.

Bois, F., and Maszle, D. 1997. MCSIM: a simulation program. *J. Stat. Software* 2(9). Available at http://toxi.ineris.fr/activites/toxicologie_quantitative/mcsim/article3

Clewell, H.J., Gentry, P.R., Allen, B.C., Covington, T.R., and Gearhart, J.M., Development of a physiologically based pharmacokinetic model of trichloroethylene and its metabolites for use in risk assessment. *Environ. Health Perspect.*, 108((suppl 2)), 283-305, 2000.

Fisher, J.W., Gargas, M.L., Allen, B.C., and Andersen, M.E. 1991. Physiologically based pharmacokinetic modeling with trichloroethylene and its metabolite, trichloroacetic acid, in the rat and mouse. *Toxicol. Appl. Pharmacol.*, 109, 183-195.

Fisher, J.W., Mahle, D.A., and Abbas, R. 1998. A human physiologically based pharmacokinetic model for trichloroethylene and its metabolites, trichloroacetic acid and free trichloroethanol. *Toxicol. Appl. Pharmacol.*, 152, 339-359.

Fisher, J.W., Physiologically based pharmacokinetic models for trichloroethylene and its oxidative metabolites. *Environ. Health Perspect.*, 108 (suppl 2), 265-273, 2000.

Gelman, A. 1996. Inference and monitoring convergence. In Markov chain Monte Carlo in practice. pp 131-143. W. R. Gilks, S. Richardson, and D. J. Spiegelhalter, eds. Chapman & Hall/CRC, Boca Raton, FL.

Gelman, A., Bois, F., and Jiang, J. 1996. Physiological Pharmacokinetic Analysis Using Population Modeling and Informative Prior Distributions. *J. Am. Stat. Assoc.* 91(436):1400-1412.

Gilks, W.R., Richardson, S., Spiegelhalter, D.J. 1996. Markov Chain Monte Carlo in Practice. Chapman & Hall/CRC, Boca Raton, FL.

Greenberg, M.S., Burton, G.A., and Fisher, J.W. 1999. Physiologically based pharmacokinetic modeling of inhaled trichloroethylene and its oxidative metabolites in B6C3F1 mice. *Toxicol. Appl. Pharmacol.*, 154, 264-278.

Larson, J.L. and Bull, R.J. 1992. Species differences in the metabolism of trichloroethylene to the carcinogenic metabolites trichloroacetate and dichloroacetate. *Toxicol. Appl. Pharmacol.*, 115, 278-285.

Lipscomb JL, Fisher JW, Confer PD, Byczkowski JZ. 1998. *In Vitro* to *in Vivo* Extrapolation of Trichloroethylene Metabolism in Humans. *Toxicol. Appl. Pharmacol.*, 152, 376-387.

Lumpkin, M. 2004. Personal communication with Dr. Lumpkin on variability of TCA binding parameters in mice, rats, and humans. (Clayton Group Services, Inc., Kennesaw, Georgia).

Prout, M.S., Provan, W.M., and Green, T. 1985. Species differences in response to trichloroethylene. *Toxicol. Appl. Pharmacol.*, 79, 389-400.

Templin, M.V., Parker, J.C., and Bull, R.J. 1993. Relative formation of dichloroacetate and trichloroacetate from trichloroethylene in male B6C3F1 mice. *Toxicol. Appl. Pharmacol.*, 123, 1-8.

Templin, M.V., Stevens, D.K., Stenner, R.D., Bonate, P.L., Tuman, D., and Bull, R.J. 1995. Factors affecting species differences in the kinetics of metabolites of trichloroethylene. *J. Toxicol. Environ. Health*, 44, 435-447.

Table 1. Summary statistics of rat prior and posterior parameter distribution for TCE. Means and standard deviations are arithmetic for cardiac output, blood flows, volumes, and fraction of blood as plasma. Values for prior and posterior mean distributions are geometric. Values for posterior standard deviation (sd) are log-scale for kinetic parameters, VPR, and partition coefficients.

	Model	Prior mean		Posterior mean		Posterior sd	
Parameter	Variable	mean	sd	mean	sd	mean	sd
Kinetic Parameters							
Oxidative clearance of TCE (VMaxC/KM)	ClC	4.48E+01	6.01E+00	1.20E+01	1.57E+00	7.57E-01	2.92E-01
Oxidative affinity (mg/L)	KM	2.50E-01	3.56E+00	4.72E-01	1.57E+00	7.31E-01	3.06E-01
Production of DCVC(/hr)	kDCVCC	1.50E-02	3.56E+00	1.27E-02	1.96E+00	4.91E-01	2.00E-01
Fractional split of TCE to TCA	FracTCE	4.00E-02	3.56E+00	4.63E-02	1.63E+00	5.27E-01	1.96E-01
Fractional split of TCE to DCA	FracDCA	4.00E-02	3.56E+00	6.15E-02	2.33E+00	5.39E-01	2.38E-01
Intrinsic Clearance producing Chloral	ClClaraC	1.20E+00	6.01E+00	2.08E+00	2.71E+00	5.78E-01	2.97E-01
Chloral production KM	KMClara	2.50E-01	3.56E+00	3.52E-01	2.06E+00	5.23E-01	2.24E-01
Protein/TCA dissociation constant (umole/L)	kDissoc	3.84E+02	1.22E+00	3.87E+02	1.09E+00	2.47E-01	4.99E-02
Number of binding sites per class protein	NumSites	1.49E+00	1.08E+00	1.49E+00	1.05E+00	1.87E-01	3.39E-02
Protein concentration (umoles/L)	ProtConc	1.90E+02	3.56E+00	1.12E+02	1.96E+00	5.24E-01	2.25E-01
Intrinsic Clearance to TCA	ClTCOHC	4.80E-01	6.01E+00	1.90E-01	2.27E+00	6.08E-01	2.98E-01
KM for oxidation to TCA	KMTCOH	2.50E-01	3.56E+00	3.75E-01	2.17E+00	5.24E-01	2.32E-01
Intrinsic Clearance for glucuronidation of TCOH	ClGlucC	4.00E+00	6.01E+00	1.16E+01	1.61E+00	5.50E-01	2.33E-01
KM for glucuronidation to TCOG	KMGluc	2.50E+01	3.56E+00	2.33E+01	2.06E+00	5.22E-01	2.25E-01
Clearance of DCVC by NAT	kNATC	1.10E+00	3.56E+00	1.02E+00	1.98E+00	4.77E-01	1.95E-01
Kidney cytotoxicity from DCVC	kKidCytoC	1.70E+01	3.56E+00	2.05E+01	1.86E+00	4.87E-01	2.04E-01
Stomach to duodenum	kTSD	1.00E+01	3.56E+00	1.81E+01	1.70E+00	5.32E-01	2.38E-01
Duodenum to liver	kAD	3.00E-01	3.56E+00	2.34E-01	1.33E+00	6.24E-01	1.98E-01
Biliary excretion of TCOG	kBileC	1.00E+00	3.56E+00	8.66E-01	1.78E+00	6.03E-01	2.60E-01
Enterohepatic recirculation of TCOH	kEHRC	1.50E-01	3.56E+00	4.37E-01	1.59E+00	4.72E-01	2.00E-01
Urinary excretion of TCA	kUrnTCAC	3.00E-01	3.56E+00	3.86E-01	1.41E+00	6.05E-01	2.14E-01
Urinary excretion of TCOG	kUrnTCOGC	5.00E-01	3.56E+00	8.18E-01	1.66E+00	5.75E-01	2.34E-01
Conversion from TCA in plasma to blood	TCAPlas	7.60E-01	3.56E+00	3.57E-01	1.37E+00	4.01E-01	1.27E-01
Alveolar ventrilation rate	VPR	1.60E+00	1.51E+00	1.63E+00	1.14E+00	2.85E-01	6.74E-02
Cardiac output	QCC	1.50E+01	4.50E+00	1.39E+01	1.63E+00	4.16E+00	9.24E-01
Fractional Blood Flows							
Fat	QFatC	7.00E-02	2.80E-02	7.51E-02	1.11E-02	2.29E-02	5.76E-03
GI tract	QGutC	1.62E-01	4.86E-02	1.57E-01	2.11E-02	4.77E-02	1.09E-02
Liver	QLivC	2.10E-02	6.30E-03	2.08E-02	2.76E-03	6.14E-03	1.40E-03
Slowly perfused tissues	QSlwC	3.36E-01	1.01E-01	3.33E-01	4.43E-02	9.77E-02	2.20E-02
Tracheobronchial region	QTBC	2.10E-02	1.65E-02	2.65E-02	7.14E-03	8.42E-03	2.64E-03
Fractional Volumes							
Fat	VFatC	7.00E-02	2.80E-02	8.28E-02	1.08E-02	2.32E-02	5.93E-03
GI tract	VGutC	2.70E-02	5.40E-03	2.70E-02	2.39E-03	6.68E-03	1.37E-03
Liver	VLivC	3.40E-02	6.80E-03	3.39E-02	3.00E-03	8.33E-03	1.67E-03
Richly perfused tissues	VRapC	1.52E-01	3.03E-02	1.52E-01	1.32E-02	3.73E-02	7.61E-03
Tracheobronchial region	VTBC	5.00E-04	1.00E-04	5.00E-04	4.33E-05	1.24E-04	2.55E-05
Blood	VBldC	7.40E-02	2.22E-02	7.30E-02	9.66E-03	2.16E-02	4.95E-03
Fraction of blood that is plasma	FracPlas	5.80E-01	1.74E-01	5.77E-01	7.60E-02	1.70E-01	3.94E-02
Volume of body for TCA distribution	VBodC	9.20E-02	7.22E-02	1.10E-01	3.15E-02	3.80E-02	1.22E-02
Volume of distribution for TCOH	VDTCOHC	6.50E-01	5.10E-01	8.23E-01	2.29E-01	2.64E-01	8.46E-02
Partition coefficients							
Blood/air	PB	1.85E+01	1.60E+00	1.62E+01	1.17E+00	3.18E-01	8.26E-02
Fat/blood	PFat	2.75E+01	1.60E+00	3.60E+01	1.19E+00	3.70E-01	9.97E-02
Gut/blood	PGut	1.30E+00	1.60E+00	1.28E+00	1.26E+00	3.61E-01	9.80E-02
Liver/blood	PLiv	1.30E+00	1.60E+00	1.30E+00	1.26E+00	3.61E-01	1.01E-01
Richly perfused/blood	PRap	1.30E+00	1.60E+00	1.38E+00	1.26E+00	3.62E-01	9.85E-02
Slowly perfused/blood	PSlw	5.00E-01	1.60E+00	5.54E-01	1.26E+00	3.62E-01	9.94E-02
Tracheobronchial/blood	PTB	1.30E+00	1.60E+00	1.30E+00	1.26E+00	3.58E-01	9.85E-02
TCA body/free in plasma	PBodTCA	5.10E-01	1.60E+00	5.10E-01	1.25E+00	3.62E-01	9.80E-02
TCA liver/free in plasma	PLivTCA	7.60E-01	1.60E+00	7.38E-01	1.25E+00	3.63E-01	9.91E-02

Table 2. Summary statistics of mouse prior and posterior parameter distribution for TCE. Means and standard deviations are arithmetic for cardiac output, blood flows, volumes, and fraction of blood as plasma. Values for prior and posterior mean distributions are geometric. Values for posterior sd are log-scale for kinetic parameters, VPR, and partition coefficients.

	Model	Prior mean		Posterior mean		Posterior sd	
Parameter	Variable	mean	sd	mean	sd	mean	sd
Kinetic Parameters							
Oxidative clearance of TCE (VMaxC/KM)	ClC	1.31E+02	6.01E+00	2.12E+02	1.66E+00	4.17E-01	1.43E-01
Oxidative affinity (mg/L)	KM	2.50E-01	3.56E+00	2.14E-01	1.67E+00	4.86E-01	1.76E-01
Production of DCVC(/hr)	kDCVCC	1.50E-02	3.56E+00	1.42E-02	2.10E+00	5.14E-01	2.21E-01
Fractional split of TCE to TCA	FracTCE	3.50E-02	3.56E+00	4.05E-02	1.68E+00	5.24E-01	2.20E-01
Fractional split of TCE to DCA	FracDCA	4.00E-02	3.56E+00	4.49E-02	2.10E+00	5.26E-01	2.22E-01
Intrinsic Clearance producing Chloral	ClClaraC	1.20E+01	6.01E+00	8.15E+00	2.69E+00	5.68E-01	2.83E-01
Chloral production KM	KMClara	2.50E-01	3.56E+00	2.67E-01	2.16E+00	5.16E-01	2.09E-01
Protein/TCA dissociation constant (umole/L)	kDissoc	4.61E+01	1.22E+00	4.60E+01	1.09E+00	2.46E-01	4.94E-02
Number of binding sites per class protein	NumSites	1.70E-01	1.08E+00	1.70E-01	1.04E+00	1.88E-01	3.46E-02
Protein concentration (umoles/L)	ProtConc	1.96E+02	3.56E+00	2.05E+02	1.85E+00	5.23E-01	2.27E-01
Intrinsic Clearance to TCA	ClTCOHC	4.00E+00	6.01E+00	6.91E+00	1.95E+00	7.29E-01	3.35E-01
KM for oxidation to TCA	KMTCOH	2.50E-01	3.56E+00	1.96E-01	1.82E+00	4.90E-01	1.96E-01
Intrinsic Clearance for glucuronidation of TCOH	ClGlucC	4.00E+00	6.01E+00	4.20E+00	1.46E+00	4.65E-01	1.93E-01
KM for glucuronidation to TCOG	KMGluc	2.50E+01	3.56E+00	3.64E+01	1.81E+00	5.03E-01	2.09E-01
Stomach to duodenum	kTSD	1.00E+01	3.56E+00	1.93E+01	1.78E+00	5.27E-01	2.34E-01
Duodenum to liver	kAD	6.00E-01	3.56E+00	8.34E-01	1.52E+00	6.54E-01	2.44E-01
Biliary excretion of TCOG	kBileC	1.00E+00	3.56E+00	4.54E-01	1.67E+00	4.74E-01	1.92E-01
Enterohepatic recirculation of TCOH	kEHRC	1.50E-01	3.56E+00	1.43E-01	2.21E+00	5.19E-01	2.29E-01
Urinary excretion of TCA	kUrnTCAC	3.00E-01	3.56E+00	5.17E-01	1.49E+00	5.03E-01	1.88E-01
Urinary excretion of TCOG	kUrnTCOGC	5.00E-01	3.56E+00	1.25E+00	1.78E+00	4.61E-01	1.76E-01
Conversion from TCA in plasma to blood	TCAPlas	7.60E-01	3.56E+00	3.78E-01	1.34E+00	3.75E-01	1.16E-01
Alveolar ventrilation rate	VPR	1.00E+00	1.51E+00	1.11E+00	1.14E+00	3.41E-01	8.81E-02
Cardiac output	QCC	1.50E+01	4.50E+00	1.79E+01	1.48E+00	4.09E+00	9.33E-01
Fractional Blood Flows							
Fat	QFatC	7.00E-02	2.80E-02	7.50E-02	1.17E-02	2.32E-02	5.84E-03
GI tract	QGutC	1.62E-01	4.86E-02	1.84E-01	1.83E-02	4.80E-02	1.10E-02
Liver	QLivC	2.10E-02	6.30E-03	2.16E-02	2.78E-03	6.14E-03	1.41E-03
Slowly perfused tissues	QSlwC	3.36E-01	1.01E-01	3.35E-01	4.52E-02	9.88E-02	2.25E-02
Tracheobronchial region	QTBC	2.10E-02	1.65E-02	2.72E-02	7.32E-03	8.52E-03	2.77E-03
Fractional Volumes							
Fat	VFatC	7.00E-02	2.80E-02	6.77E-02	1.08E-02	2.59E-02	6.15E-03
GI tract	VGutC	2.70E-02	5.40E-03	2.70E-02	2.36E-03	6.65E-03	1.34E-03
Liver	VLivC	3.40E-02	6.80E-03	3.39E-02	3.08E-03	8.40E-03	1.72E-03
Richly perfused tissues	VRapC	1.52E-01	3.03E-02	1.51E-01	1.31E-02	3.73E-02	7.48E-03
Tracheobronchial region	VTBC	5.00E-04	1.00E-04	4.99E-04	4.32E-05	1.22E-04	2.46E-05
Blood	VBldC	7.40E-02	2.22E-02	7.55E-02	9.80E-03	2.18E-02	5.03E-03
Fraction of blood that is plasma	FracPlas	5.80E-01	1.74E-01	5.87E-01	7.50E-02	1.71E-01	3.91E-02
Volume of body for TCA distribution	VBodC	9.20E-02	7.22E-02	1.05E-01	3.04E-02	3.70E-02	1.17E-02
Volume of distribution for TCOH	VDTCOHC	6.50E-01	5.10E-01	9.66E-01	2.00E-01	2.61E-01	8.45E-02
Partition coefficients							
Blood/air	PB	1.85E+01	1.60E+00	1.64E+01	1.18E+00	3.41E-01	9.29E-02
Fat/blood	PFat	2.75E+01	1.60E+00	3.47E+01	1.20E+00	4.25E-01	1.02E-01
Gut/blood	PGut	1.30E+00	1.60E+00	1.77E+00	1.25E+00	3.58E-01	9.85E-02
Liver/blood	PLiv	1.30E+00	1.60E+00	1.81E+00	1.26E+00	3.58E-01	9.81E-02
Richly perfused/blood	PRap	1.30E+00	1.60E+00	1.80E+00	1.27E+00	3.61E-01	9.83E-02
Slowly perfused/blood	PSlw	5.00E-01	1.60E+00	7.62E-01	1.26E+00	3.56E-01	9.79E-02
Tracheobronchial/blood	PTB	1.30E+00	1.60E+00	1.82E+00	1.26E+00	3.62E-01	9.73E-02
TCA body/free in plasma	PBodTCA	5.10E-01	1.60E+00	7.58E-01	1.25E+00	3.53E-01	9.33E-02
TCA liver/free in plasma	PLivTCA	7.60E-01	1.60E+00	1.11E+00	1.26E+00	3.58E-01	9.74E-02

Table 3. Summary statistics of human prior and posterior parameter distribution for TCE. Means and standard deviations are arithmetic for cardiac output, blood flows, volumes, and fraction of blood as plasma. Values for prior and posterior mean distributions are geometric. Values for posterior sd are log-scale for kinetic parameters, VPR, and partition coefficients.

	Model	Prior mean		Posterior mean		Posterior sd	
Parameter	Variable	mean	sd	mean	sd	mean	sd
Kinetic Parameters							
Oxidative clearance of TCE (VMaxC/KM)	ClC	9.00E+00	2.00E+00	5.52E+00	1.28E+00	3.91E-01	1.41E-01
Oxidative affinity (mg/L)	KM	2.30E+01	2.00E+00	1.90E+01	1.39E+00	7.14E-01	2.62E-01
Production of DCVC(/hr)	kDCVCC	1.50E-02	3.56E+00	9.31E-03	1.96E+00	5.14E-01	2.40E-01
Fractional split of TCE to TCA	FracTCE	8.00E-02	3.56E+00	2.36E-01	1.32E+00	3.99E-01	1.37E-01
Fractional split of TCE to DCA	FracDCA	4.00E-03	3.56E+00	4.11E-03	2.46E+00	5.64E-01	2.83E-01
Intrinsic Clearance producing Chloral	ClClaraC	3.00E-03	6.01E+00	3.13E-03	3.40E+00	6.11E-01	3.51E-01
Chloral production KM	KMClara	1.50E+00	3.56E+00	1.60E+00	2.35E+00	5.63E-01	2.88E-01
Protein/TCA dissociation constant (umole/L)	kDissoc	1.75E+02	1.08E+00	1.74E+02	1.06E+00	2.62E-01	7.25E-02
Number of binding sites per class protein	NumSites	2.97E+00	1.02E+00	2.97E+00	1.02E+00	2.45E-01	6.77E-02
Protein concentration (umoles/L)	ProtConc	2.39E+02	3.56E+00	2.13E+02	1.71E+00	4.98E-01	2.22E-01
Intrinsic Clearance to TCA	ClTCOHC	1.00E-01	6.01E+00	5.25E-02	1.40E+00	5.40E-01	2.25E-01
KM for oxidation to TCA	KMTCOH	2.50E+02	3.56E+00	1.95E+02	2.48E+00	5.79E-01	3.03E-01
Intrinsic Clearance for glucuronidation of TCOH	ClGlucC	2.00E-01	6.01E+00	1.80E-01	1.35E+00	4.01E-01	1.38E-01
KM for glucuronidation to TCOG	KMGluc	2.50E+01	3.56E+00	7.77E+01	1.69E+00	5.01E-01	2.31E-01
Clearance of DCVC by NAT	kNATC	1.90E+01	3.56E+00	1.44E+01	2.19E+00	5.35E-01	2.58E-01
Kidney cytotoxicity from DCVC	kKidCytoC	3.70E+01	3.56E+00	5.00E+01	2.14E+00	5.26E-01	2.52E-01
Biliary excretion of TCOG	kBileC	1.00E+00	3.56E+00	2.65E+00	2.20E+00	6.12E-01	3.23E-01
Enterohepatic recirculation of TCOH	kEHRC	1.00E-02	3.56E+00	1.13E-02	2.46E+00	5.70E-01	2.88E-01
Urinary excretion of TCA	kUrnTCAC	2.00E-01	3.56E+00	2.43E-01	1.46E+00	4.51E-01	1.76E-01
Urinary excretion of TCOG	kUrnTCOGC	3.00E+00	3.56E+00	9.72E+00	1.62E+00	4.68E-01	1.81E-01
Conversion from TCA in plasma to blood	TCAPlas	7.60E-01	3.56E+00	5.46E-01	1.32E+00	3.93E-01	1.52E-01
Alveolar ventrilation rate	VPR	1.38E+00	1.51E+00	2.21E+00	1.18E+00	3.54E-01	1.16E-01
Cardiac output	QCC	1.30E+01	3.90E+00	1.59E+01	1.91E+00	4.38E+00	1.47E-01
Fractional Blood Flows							
Fat	QFatC	5.20E-02	2.08E-02	6.13E-02	1.16E-02	1.97E-02	8.46E-04
GI tract	QGutC	1.81E-01	5.43E-02	2.09E-01	2.89E-02	6.30E-02	2.24E-03
Liver	QLivC	4.60E-02	1.38E-02	5.39E-02	7.33E-03	1.57E-02	5.52E-04
Slowly perfused tissues	QSlwC	2.49E-01	7.47E-02	1.77E-01	3.54E-02	8.42E-02	3.10E-03
Tracheobronchial region	QTBC	2.50E-02	1.96E-02	3.06E-02	1.05E-02	1.17E-02	8.76E-04
Volumes							
Body Weight	BW	7.00E+01	3.39E+00	5.99E+01	1.52E+00	4.88E-01	2.21E-01
Fat	VFatC	2.14E-01	8.56E-02	2.09E-01	5.04E-02	8.43E-02	4.03E-03
GI tract	VGutC	1.70E-02	3.40E-03	1.61E-02	2.03E-03	5.36E-03	1.36E-04
Liver	VLivC	2.60E-02	5.20E-03	2.31E-02	2.96E-03	8.08E-03	2.24E-04
Richly perfused tissues	VRapC	1.48E-01	2.96E-02	1.37E-01	1.79E-02	4.67E-02	1.29E-03
Tracheobronchial region	VTBC	8.00E-04	1.60E-04	7.99E-04	9.79E-05	2.52E-04	6.68E-06
Blood	VBldC	7.90E-02	2.37E-02	7.56E-02	1.33E-02	2.75E-02	9.08E-04
Fraction of blood that is plasma	FracPlas	5.80E-01	1.74E-01	5.85E-01	9.86E-02	2.04E-01	6.72E-03
Volume of body for TCA distribution	VBodC	9.20E-02	7.22E-02	1.49E-01	2.83E-02	4.22E-02	2.73E-03
Volume of distribution for TCOH	VDTCOHC	6.50E-01	5.10E-01	7.95E-01	1.71E-01	2.74E-01	1.42E-02
Partition coefficients							
Blood/air	PB	9.20E+00	1.60E+00	8.79E+00	1.20E+00	4.08E-01	1.30E-01
Fat/blood	PFat	7.30E+01	1.60E+00	6.48E+01	1.32E+00	4.29E-01	1.55E-01
Gut/blood	PGut	6.80E+00	1.60E+00	4.73E+00	1.25E+00	3.98E-01	1.41E-01
Liver/blood	PLiv	6.80E+00	1.60E+00	5.43E+00	1.25E+00	4.74E-01	1.64E-01
Richly perfused/blood	PRap	6.80E+00	1.60E+00	4.54E+00	1.24E+00	3.85E-01	1.40E-01
Slowly perfused/blood	PSlw	2.30E+00	1.60E+00	3.62E+00	1.23E+00	3.81E-01	1.39E-01
Tracheobronchial/blood	PTB	6.80E+00	1.60E+00	6.73E+00	1.32E+00	4.12E-01	1.49E-01
TCA body/free in plasma	PBodTCA	1.90E+00	1.60E+00	2.38E+00	1.29E+00	4.32E-01	1.57E-01
TCA liver/free in plasma	PLivTCA	2.50E+00	1.60E+00	1.68E+00	1.24E+00	3.85E-01	1.42E-01